

A Preliminary Detection of Arcminute Scale Cosmic Microwave Background Anisotropy with the BIMA Array

K.S. Dawson¹, W.L. Holzapfel¹, J.E. Carlstrom²,
M. Joy³, S.J. LaRoque² and E.D. Reese²

ABSTRACT

We have used the Berkeley-Illinois-Maryland-Association (BIMA) array outfitted with sensitive cm-wave receivers to expand our search for arcminute scale anisotropy of the Cosmic Microwave Background (CMB). The interferometer was placed in a compact configuration to obtain high brightness sensitivity on arcminute scales over its 6.6' FWHM field of view. The sensitivity of this experiment to flat band power peaks at a multipole of $\ell = 5530$ which corresponds to an angular scale of $\sim 2'$. We present the analysis of a total of 470 hours of on-source integration time on eleven independent fields which were selected based on their low IR dust contrast and lack of bright radio sources. Applying a Bayesian analysis to the visibility data, we find CMB anisotropy flat-band power $Q_{flat} = 6.1_{-4.8}^{+2.8} \mu\text{K}$ at 68% confidence. The confidence of a non-zero signal is 76% and we find an upper limit of $Q_{flat} < 12.4 \mu\text{K}$ at 95% confidence. We have supplemented our BIMA observations with concurrent observations at 4.8 GHz with the VLA to search for and remove point sources. We find that point sources make an insignificant contribution to the observed anisotropy.

Subject headings: cosmology: observation – cosmic microwave background

¹Department of Physics, University of California, Berkeley CA 94720

²Department of Astronomy and Astrophysics, University of Chicago, Chicago IL 60637

³Space Science Laboratory, SD50, NASA Marshall Space Flight Center, Huntsville AL 35812

1. Introduction

The Cosmic Microwave Background (CMB) radiation carries a wealth of information about the early universe. In the standard inflationary model, the distribution of matter at the epoch of recombination leads to small temperature anisotropy of the CMB. Measurement of anisotropy on the largest angular scales reveals the primordial distribution of matter (Smoot et al. 1992). Structures which came into the horizon and were able to collapse near the epoch of recombination lead to anisotropy at degree angular scales. The resulting CMB anisotropy angular power spectrum at these scales is highly sensitive to the parameters of the cosmological model. Measurements of degree scale anisotropy have been made, for example, to constrain the curvature of the universe (Miller et al. 1999, deBernardis et al. 2000, Hanany et al. 2000). The anisotropy on smaller angular scales, less than a few arcminutes, will be exponentially damped to vanishingly small levels due to photon diffusion and from the finite thickness of the ‘surface’ of last scattering (Hu & White 1997). At arcminute scales, so-called secondary anisotropy generated by the reionization of the universe and the Sunyaev-Zel’dovich effect from galaxy clusters should dominate the primary signal (for a review see Haiman & Knox 1999).

In this paper we report results from our ongoing program using the Berkeley Illinois Maryland Association (BIMA) interferometer to search for arcminute-scale CMB anisotropy. Discussion of the instrument, data reduction, Bayesian maximum likelihood analysis, expected signals (from both primary and secondary anisotropies) and comparison with previous experiments is included in the release of our earlier results (Holzapfel et al. 2000). The field selection and observations are reviewed in §2. The results of the Bayesian analysis are presented in §3 including a discussion of the effects of point source subtraction. Finally, in §4, we summarize the results of the survey.

2. Observations

We have used the BIMA array at 28.5 GHz during the summers of 1997, 1998 and 2000 to search for CMB anisotropy. We observed seven independent fields over the course of the first two summers. In two of these fields we found apparent detections of excess power. We extended our observations of those two fields in the summer of 2000 and also added four new fields to the survey.

2.1. Field Selection

For observations in the summer of 2000, we selected four new fields, each located within 2° of one of the fields selected in 1998. We employed such a strategy to make efficient use of observing time allowing a six hour separation between fields as in the 1998 survey, and to search for systematic errors which could have resulted in false detections in our previous observations. The new fields were chosen to lie in regions of low dust emission and contrast as determined from examination of IRAS $100\ \mu\text{m}$ maps. The VLA NVSS (Condon et al. 1998) and FIRST (White et al. 1997) surveys were then used to select regions free of bright point sources at 1.4 GHz. In addition, we used the SkyView digitized sky survey and ROSAT WFC maps to check for bright optical or x-ray emission which could complicate follow-up observations. The pointing centers for each of the six fields observed in the summer of 2000 are given in Table 1.

2.2. BIMA Observations

All anisotropy observations were made using the BIMA array at Hat Creek. The array consists of nine 6.1 meter telescopes operating at 28.5 GHz, each with a $6.6'$ FWHM primary beam. In order to track the system gains, each 25 minute source observation was bracketed by a 5 minute observation of a calibrator. The fluxes of the calibration sources are all referenced to the flux of Mars which is uncertain by approximately 4% at 90% confidence (see discussion in Grego 1999). Of the total time spent observing, $\sim 60\%$ was spent on source. The cumulative integration times for each of the 6 fields observed in 2000 are listed in Table 1. Combined with the observations described in Holzapfel et al. 2000, a total of 470 hours of on-source integration have been dedicated to this project.

2.3. VLA Observations and Point Source Results

The compact configuration used for the 2000 Summer BIMA anisotropy observations produced high brightness sensitivity but lacked the spatial dynamic range to distinguish point sources from CMB fluctuations. To constrain the contribution from point sources to our anisotropy measurements, we therefore used the Very Large Array (VLA) to survey each of the new fields as well as two of the 1998 fields which lacked point source observations. The 4.8 GHz

VLA observations were obtained within a month of the 2000 Summer BIMA observations. With an hour and a half of observing time per field, we reached an RMS flux of $\sim 25\text{--}30\ \mu\text{Jy}$ at the center of a $9'$ FWHM region centered on each of the blank fields observed with BIMA.

In the 6 fields examined with the VLA, we found 18 point sources with fluxes adjusted for the attenuation of the primary beam ranging from $157\ \mu\text{Jy}$ to $2000\ \mu\text{Jy}$. The average flux of these point sources was $743\ \mu\text{Jy}$.

The point source model at 28.5 GHz is extrapolated from the lower frequency VLA data by assuming a spectral index of $\alpha = -0.71$ where $S_\nu \propto \nu^\alpha$ (Cooray et al. 1998). After accounting for attenuation due to the BIMA primary beam, all of the point sources detected with the VLA are expected to be near or below the measured RMS flux density achieved in the BIMA blank field data.

3. Results

We have produced and analyzed images for each of the observed fields. The statistics of the images produced with only the short baselines used in the likelihood analysis are listed in Table 2. The observed RMS values are comparable to those expected from the noise properties of the visibilities. We also express our results in terms of the RMS Rayleigh-Jeans (RJ) temperature fluctuations.

3.1. Anisotropy Analysis

We use the method described in Holzapfel et al. (2000) to determine the relative likelihoods that the observed fields are described by a model for the CMB fluctuations with flat band power Q_{flat} . We present the results of the data analysis of the BIMA data both with and without the subtraction of the point sources extrapolated from the VLA observations. In Table 3, we show the most likely Q_{flat} for each of the fields observed in the summer of 2000 with no point source subtraction.

Figure 1 shows the relative likelihoods as a function of assumed Q_{flat} in each of the fields observed in the summer of 2000 with no point source subtraction. The results are normalized to unity likelihood for the case of no anisotropy signal. Note that the results for fields BDF6 and BDF7 as displayed in both Table 3 and Figure 1 also include the data collected in the summer of 1998.

We estimate the point source contribution to the BIMA results by extrapolating the flux of point sources detected with the VLA at 4.8 GHz to the 28.5 GHz BIMA observation frequency assuming spectral index α . These sources are then removed from the raw data by taking the Fourier transform of the point source model modulated by the primary beam response and subtracting it directly from the visibility data. In Figure 2, we plot the combined likelihood for all of the fields under three assumptions for subtracted point source model; no point sources, extrapolated fluxes assuming $\alpha = -0.71$, and a flat spectrum ($\alpha = 0$) for all sources. In Table 4, we list the 68% and 95% confidence intervals in Q_{flat} for each of the three point source extrapolations we have considered. The results are identical before and after the subtraction of the source fluxes estimated assuming $\alpha = -0.71$. Assuming a flat spectrum, the most likely Q_{flat} slightly increases indicating that we have overestimated the flux of the point sources and by subtracting these sources we are adding excess power to the BIMA data. It is clear that point sources cannot account for the detected excess power.

Again, as found in Holzapfel et al. (2000), the joint likelihood for all the data, shown in Figure 2, peaks at $Q_{flat} > 0$. While the most likely Q_{flat} remains essentially unchanged from the earlier results, the addition of the new observations has increased the significance of the detection. When no point sources are subtracted, the confidence of a non-zero Q_{flat} for the joint likelihood is 76% which can be compared with 44% for the total of all data collected prior to the summer 2000 observations.

3.2. Systematics Check

Much of the motivation for the new BIMA observations described here was to perform tests for systematic errors that could have been responsible for the previously reported detections. We first investigated if the observed excess power could somehow depend on the position of the source on the sky. As described in Section 2.1, we selected the four new fields to lie within two degrees of the four fields selected for observation in 1998. The results for the two 18 hour right ascension fields, BDF6 and BDF10, were compared. Observations in 2000 repeated the detection of excess power in BDF6, but none was found in BDF10 indicating that the observed excess power in BDF6 is not due to a systematic associated with sky position. For the two 7 hour right ascension fields, BDF7 and

BDF11, the results are not as conclusive; excess power was detected in both fields. To check for possibility of coherent power between the fields, e.g., possibly from a local source of interference, we analyzed the data from the two fields as if they were from the same position on the sky. No coherent signal was detected; the level of the detected power decreased.

We have performed several additional tests of the data to search for systematic errors in the fields in which we find excess power. Since the data on each field was collected over an extended period of time, we divided the data into blocks of several days and analyzed each block independently. If we were experiencing problems over a short period of time, we might expect to find a significantly larger detection in one of the blocks of data. None was found. We next checked for the presence of systematic errors as a function of time of day. For each field, we divided the data into three blocks spanning equal intervals in hour angle. Again, there was no evidence for anomalous excess power in any of the blocks of data. Although we see no convincing evidence that our determination of excess power is the result of a systematic error, higher sensitivity observations will be necessary to eliminate this possibility.

4. Conclusion

Over the course of three summers, we have used the BIMA array in a compact configuration at 28.5 GHz to search for CMB anisotropy in eleven independent $6'.6$ FWHM fields. With these observations, we have made a preliminary detection of arcminute scale CMB anisotropy. In the context of an assumed flat band power model for the CMB power spectrum, we find $Q_{flat} = 6.1^{+2.8}_{-4.8} \mu\text{K}$ at 68.3% confidence with sensitivity on scales that correspond to an average harmonic multipole $\ell_{eff} = 5530$. The confidence of a non-zero signal is 76% and we find an upper limit of $Q_{flat} < 12.4 \mu\text{K}$ at 95% confidence. The 28.5 GHz fluxes of the point sources located with the VLA are near or below the noise level in the BIMA images and make no significant contribution when included in the likelihood analysis. A recent search for CMB anisotropy on similar angular scales with the ATCA at 8.7 GHz (Subrahmanyam et al. 2000) was able to place an upper limit of $Q_{flat} < 25 \mu\text{K}$ at 95% confidence, but this work was believed to be confusion limited by unresolved point sources. We can use our VLA 5σ flux limit of $\sim 150 \mu\text{Jy}$ at 4.8 GHz to es-

timate the contribution of unresolved point sources to the excess power we report. Assuming a universal spectral index of $\alpha = -0.71$, we expect a contribution of $Q_{flat} \sim 1.1 \mu\text{K}$ due to unresolved point sources in the BIMA data at 28.5 GHz. Assuming a flat spectral index of $\alpha = 0$, we expect a contribution of $Q_{flat} \sim 3 \mu\text{K}$ as a conservative upper limit.

This work is perhaps the first detection of secondary CMB anisotropy in a region of the sky not selected for the presence of a known galaxy cluster. A detection of excess power is not surprising when one considers the level of anisotropy expected from the SZ effect of distant clusters of galaxies. Recent hydrodynamic simulations predict a $Q_{flat} \sim 9.7 \mu\text{K}$ (Springel, White, & Hernquist 2000). Although this value is larger than our most likely fit, it falls well within our 68% confidence interval. Considering the way in which our blank fields are selected, it is not surprising to find a lower value for Q_{flat} than is predicted for randomly selected regions of the sky. The density of extragalactic radio sources is a tracer of large scale structure. By selecting fields with little point source contamination, we introduce a bias against finding clusters of galaxies. If the excess power we have detected is indeed due to the SZ effect in distant clusters of galaxies, deeper observations will resolve the individual clusters enabling a new and powerful probe of large scale structure.

This paper is dedicated to the memory of Mark Warnock, an electronics engineer at the BIMA observatory. His expertise and guidance helped ensure the success of the cm-wave imaging program at BIMA. We thank the entire staff of the BIMA observatory for their many contributions to this project. We also thank Rick Forster, Laura Grego, Daisuke Nagai and Dick Plambeck for assistance with the instrumentation and observations. This work is supported in part by NASA LTSA grant number NAG5-7986. The BIMA millimeter array is supported by NSF grant AST 96-13998. We are grateful for the scheduling of Target of Opportunity time at the VLA in support of this project.

REFERENCES

- Condon, J. J., Cotton, W. D., Greisen, E. W., Yin, Q. F., Perley, R. A. Taylor, G. B., & Broderick, J. J. 1998, *AJ*, 115, 1693.
- Cooray, A. R., Grego, L., Holzapfel, W. L., Joy, M., & Carlstrom, J. E. 1998, *AJ*, 115, 1388.
- Grego, L. 1999, Ph. D. thesis, Caltech.
- deBernardis, P. et al. 2000, *Nature*, 404, 955.
- Haiman, Z., & Knox, L. 1999, astro-ph/9902311.
- Hanany, S. et al. 2000, *ApJ*, in press.
- Holzapfel, W. L., Carlstrom, J. E., Grego, L., Holder, G., Joy, M., & Reese, E. D. 2000, *ApJ*, 539, 57.
- Hu, W., & White, M. 1997, *ApJ*, 479, 568.
- Miller, A. D., Caldwell, R., Devlin, M. J., Dorwart, W. Herbig, T., Nolta, Page, L., Puchalla, J., Torbet, E, and Tran, H. 1999, *ApJ*, 524, L1.
- Smoot, G. F. et al. 1992, *ApJ*, 396, L1.
- Springel, V., White, M., & Hernquist, L. 2000, astro-ph/0008133.
- Subrahmanyam, R., Kesteven M.J., Ekers R.D., Sinclair M., & Silk J. 2000, *MNRAS*, 315, 808.
- White, R. L., Becker, R. H., Helfand, D. J., & Gregg, M. D. 1997, *ApJ*, 475, 479.

TABLE 1
Field Positions and Observation Times

Fields	α (J2000)	δ (J2000)	Observation year(s)	Time (Hrs)
BDF6	18 ^h 21 ^m 00.0 ^s	+59° 15' 00''	1998, 2000	81.2
BDF7	06 ^h 58 ^m 45.0 ^s	+55° 17' 00''	1998, 2000	68.2
BDF8	00 ^h 17 ^m 30.0 ^s	+29° 00' 00''	2000	34.6
BDF9	12 ^h 50 ^m 15.0 ^s	+56° 52' 30''	2000	24.5
BDF10	18 ^h 12 ^m 37.21 ^s	+58° 32' 00''	2000	14.3
BDF11	06 ^h 58 ^m 00.0 ^s	+54° 24' 00''	2000	22.1

TABLE 2
Image Statistics for u - v Range 0.63 – 1.2 k λ

Field	Beamsize('')	RMS (μ Jy beam ⁻¹)		RMS (μ K)	
		estimated	measured	estimated	measured
BDF6	106.7 \times 118.9	113	166	13.4	19.6
BDF7	108.0 \times 120.3	130	166	15.0	19.2
BDF8	102.6 \times 116.1	166	133	20.9	16.7
BDF9	101.6 \times 118.9	209	196	26.0	24.3
BDF10	105.3 \times 115.5	275	276	33.9	34.0
BDF11	104.4 \times 115.1	208	279	26.0	34.8

TABLE 3
Most Likely Q_{flat} and Confidence Intervals

Field	Most Likely	Q_{flat} (μ K)	
		68%	95%
BDF6	15.0	8.2 – 22.4	0.8 – 28.6
BDF7	13.2	3.2 – 21.2	0.0 – 31.8
BDF8	0.0	0.0 – 10.4	0.0 – 21.2
BDF9	0.0	0.0 – 15.0	0.0 – 30.6
BDF10	0.0	0.0 – 23.2	0.0 – 47.6
BDF11	23.2	10.8 – 35.6	0.0 – 46.2

TABLE 4
Analysis of Combined Fields Including Confidence of $Q_{flat} > 0$

Point source model	Most likely	Q_{flat} (μ K)		Confidence
		68%	95%	$Q_{flat} > 0$
none	6.1	1.3 – 8.9	0.0 – 12.4	76%
$\alpha = -0.71$	6.1	1.4 – 8.9	0.0 – 12.4	76%
$\alpha = 0$	7.2	2.4 – 10.5	0.0 – 13.2	85%

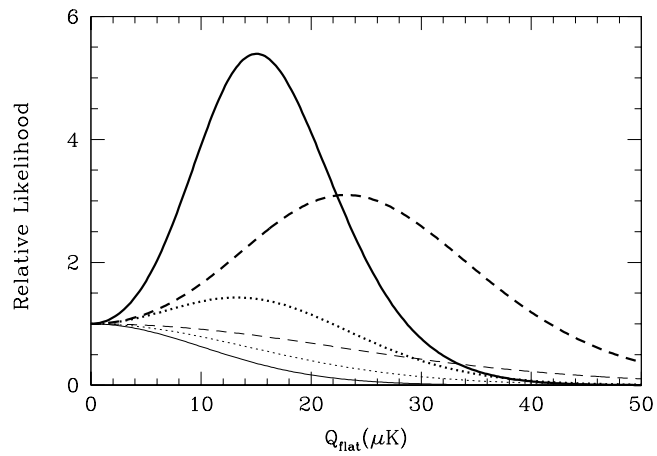


Fig. 1.— The relative likelihood that the observed signal in each field is described by flat band power with amplitude Q_{flat} ignoring possible point sources. The light solid line corresponds to field BDF08, the light dotted line to BDF09, the light dashed line to BDF10, the heavy solid line to BDF06, the heavy dotted line to BDF07, and the heavy dashed line to BDF11.

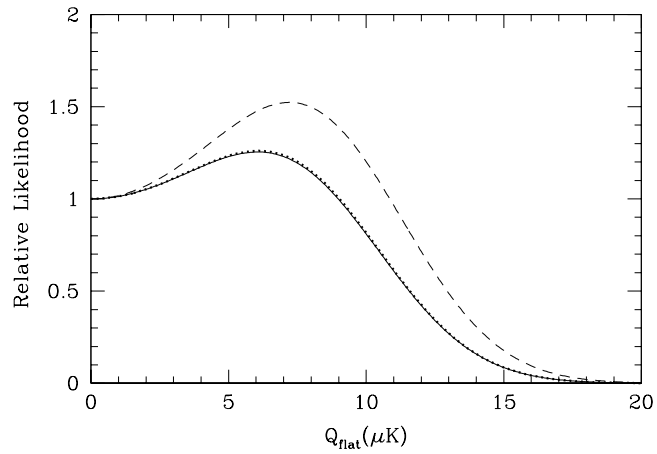


Fig. 2.— The relative likelihood that the observed signal in the combined fields is described by flat band power with amplitude Q_{flat} . The solid line corresponds to an analysis ignoring the measured point sources, the dotted line is the result of subtracting point sources assuming a spectral index of -0.71 , and the dashed line is the result of subtracting measured point sources assuming a flat spectrum.